Journal of the Korean Ceramic Society
Vol. 51, No. 4, pp. 260~264, 2014.

http://dx.doi.org/10.4191/kcers.2014.51.4.260

Terbium and Tungsten Co-doped Bismuth Oxide Electrolytes for Low Temperature Solid Oxide Fuel Cells

Doh Won Jung, Kang Taek Lee*,†, and Eric D. Wachsman,††**

Samsung Advanced Institute of Technology, Yongin 446-712, Republic of Korea
**Department of Energy Systems Engineering, DGIST (DaeguGyeongbuk Institute Science and Technology), Daegu 711-873, Republic of Korea*
***University of Maryland Energy Research Center, University of Maryland, College Park, MD 20742, USA*

(Received June 12, 2014; Revised June 29, 2014; Accepted June 30, 2014)

ABSTRACT

We developed a novel double dopant bismuth oxide system with Tb and W. When Tb was doped as a single dopant, a Tb dopant concentration more than 20 mol% was required to stabilize bismuth oxides with a high conductivity cubic structure. High temperature XRD analysis of 25 mol% Tb-doped bismuth oxide (25TSB) confirmed that the cubic structure of 25TSB was retained from room temperature to 700°C with increase in the lattice parameter. On the other hand, we achieved the stabilization of high temperature cubic phase with a total dopant concentration as low as ~12 mol% with 8 mol% Tb and 4 mol% W double dopants (8T4WSB). Moreover, the measured ionic conductivity of 10T5WSB was much higher than 25TSB, thus demonstrating the feasibility of the double dopant strategy to develop stabilized bismuth oxide systems with higher oxygen ion conductivity for the application of SOFC electrolytes at reduced temperature. In addition, we investigated the long-term stability of TSB and TWSB electrolytes.

Key words : Solid oxide fuel cells, Electrolytes, Bismuth oxides, Double dopants

1. Introduction

Solid oxide fuel cells (SOFCs) are highly efficient and eco-friendly energy conversion devices.[1,2] The major obstacles to the commercialization of this fascinating technology are high system cost and rapid performance-degradation due to high operation temperature (> 800°C).[1] Thus, lowering the operation temperature of SOFCs can considerably reduce the system cost due to the utilization of a wider range of cheap and high-performance materials. System stability can also be improved due to the increased thermo-mechanical strength and slow degradation kinetics at reduced temperature.[3,4]

However, as the temperature decreases, the ionic conduction in electrolytes and electrochemical reactions in electrodes, which are major mechanistic steps of SOFC operation, are dramatically slowed down due to their thermally activated nature, thus deteriorating the overall SOFC performance.[3,5] Therefore, the development of electrolytes with higher conductivityis of critical importance to achieve high-performance SOFCs that can operate at reduced temperature.

†Corresponding author : Kang Taek Lee
E-mail : ktlee@dgist.ac.kr
Tel : +82-53-785-6430 Fax : +82-53-785-6409
††Corresponding author : Eric D. Wachsman
E-mail : ewach@umd.edu
Tel : +1-301-405-8193 Fax : +1-301-314-8514

In this respect, bismuth oxides with a cubic structure (δ-Bi_2O_3) are attractive due to their highest oxygen ion conductivity among fluorite oxides.[6-9] The conductivity of δ-Bi_2O_3 below 800°C is more than 100 times higher than that of yttria stabilized zirconia (YSZ), which is the most prevalent SOFC electrolyte material.[10] This high conductivity of δ-Bi_2O_3 is primarily attributed to its intrinsic oxygen vacancies of 25%. However, there exists only a narrow stability window of this cubic phase (730 - 824°C), limiting its application in practical SOFC systems.[11] To overcome this issue, Takahashi *et al.* reported stabilization of the high temperature cubic phase of bismuth oxides by doping with lanthanides.[12] Verkerk *et al.* found that the highest ionic conductivity among the stabilized bismuth oxides with a single dopant was obtained by doping with Er^{3+} (20 mol%) due to the lowest dopant concentration for the stabilization of δ-Bi_2O_3.[13,14] Later, a double dopant strategy was developed to stabilize the cubic δ-Bi_2O_3 structure, and several doubly doped Bi_2O_3 electrolyte systems have been studied.[15-17] Compared to single dopant stabilization, double-dopant doping allows a much lower total dopant concentration to stabilize the fluorite phase down to room temperature due to a significant increase in entropy.[16] Recently, Wachsman *et al.* developed a novel doubly doped bismuth oxide system with Dy and W (DWSB).[8,17-19] In these studies, the minimum dopant concentration required to stabilize the cubic phase was reduced by 12 mol% (8 mol% Dy and 4 mol% W, 8D4WSB).[17] With 8D4WSB, the highest ionic conductivity was achieved (e.g., 0.57 S-cm^{-1} at 700°C), demonstrating the high feasibil-

ity of the double doping approach to enhance the ionic conductivity of stabilized bismuth oxides.

In this study, we developed Tb and W co-doped bismuth oxides. We selected Tb as a dopant since it has a slightly larger ionic radius and greater polarizability than Dy, thus expecting higher stability and conductivity compared to that of DWSB.[7]

2. Experimental Procedure

2.1. Preparation of electrolyte samples

A flow chart of the sample preparation procedure is given in Fig. 1. The doped bismuth oxide powders with various compositions were developed via a typical solid-state reaction. In this study, we prepared 5 different compositions, including $(TbO_{1.75})_x(BiO_{1.5})_{1-x}$ (where x = 0.15, 0.20, and 0.25) and $(TbO_{1.75})_x(WO_3)_y(BiO_{1.5})_{1-x-y}$ (where (x, y) = (0.08, 0.04), and (0.10, 0.05)). The first three compositions with a single dopant (Tb) are referred to as 15TSB, 20TSB, and 25TSB, respectively. The latter two samples, co-doped with Tb and W are referred to as 8T4WSB and 10T5WSB, respectively.

A stoichiometric mixture of Bi_2O_3 (99.9995%), Tb_4O_7 (99.99%) and WO_3 (99.8%), from Alfa Aesar, were ball-milled with zirconia ball media for 24 h. After milling, the powder mixtures were calcined at 800°C for 16 h and sieved with 325 mesh to achieve uniform particle sizes. The calcined powders were packed in a stainless steel die with 8 mm diameter and pressed uniaxially in the form of pellets under 40 MPa, and the subsequent cold isostatic pressing was performed at 200 MPa. The green bodies were sintered at 890°C for 16 h in ambient air. Au paste (Engelhard) was brush-painted to form electrodes on the surface of both sides of the pellets and the electrodes were sintered at 800°C for 1 h. For the current-collecting purpose, Pt wires were attached to both electrode surfaces.

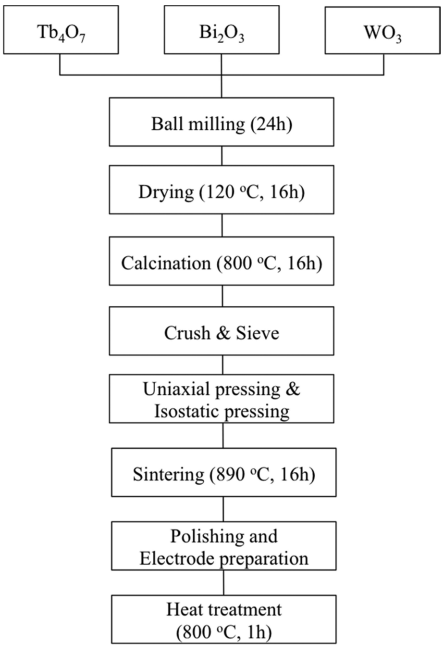

Fig. 1. Fabrication procedure of the Tb and W co-doped electrolyte samples.

2.2. X-Ray diffraction analysis

X-ray diffraction analysis (XRD, Philips APD 3720) was conducted to determine the crystal structure of the synthesized doped bismuth oxides using CuKα1 radiation between 20° and 70°(2θ) at room temperature. For better lattice parameter estimation, the high temperature XRD (HT-XRD, APD 3720 HT) from Philips was utilized under He gas in the temperature range from 25 to 700°C. The contribution of Kα2 radiation was subtracted using the ProFit software (Philips).

2.3. Conductivity measurements

The total conductivity of the samples was measured by two-point probe electrochemical impedance spectroscopy (EIS) using a Solatron 1260 with an AC voltage amplitude of 10 mV over the frequency range from 0.1 MHz to 0.1 Hz in ambient air. Data acquisition was performed with Z plot software. To avoid artifacts from the lead wires and the equipment due to inductive responses, the resistance of the lead wires measured without a testing sample was subtracted from the measured data for each sample.

3. Results and Discussion

3.1. Phase stability

Figure 2 shows the XRD patterns of the singly doped specimens, including 15TSB, 20TSB, and 25TSB. Only 25TSB exhibited a pure cubic fluorite phase (δ-Bi_2O_3), while the bismuth oxides containing 15 and 20 mol% Tb showed the coexistence of the majority of cubic and minor rhombohedral ($Bi_{1.55}Tb_{0.45}O_3$) phases. Thus, this result indicates that the stabilization of the high conductivity cubic structure of bismuth oxides requires a Tb dopant concentration higher

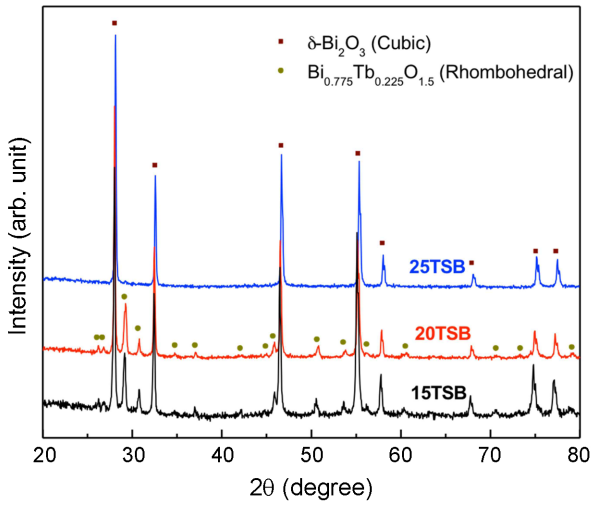

Fig. 2. XRD patterns of 15TSB, 20TSB, and 25TSB.

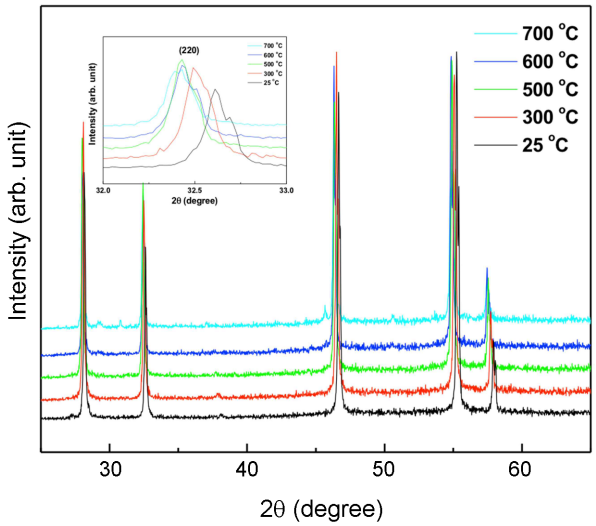

Fig. 3. HT-XRD patterns of 25TSB measured from 25 to 700°C. Inset shows a magnified region at the range of 2θ angle from 32 to 33 degrees.

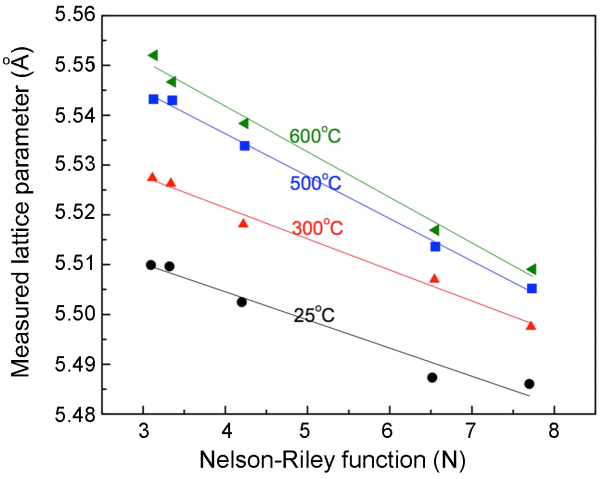

Fig. 4. Plots of the measured apparent lattice parameters as a function of the Nelson-Riley function at various temperatures.

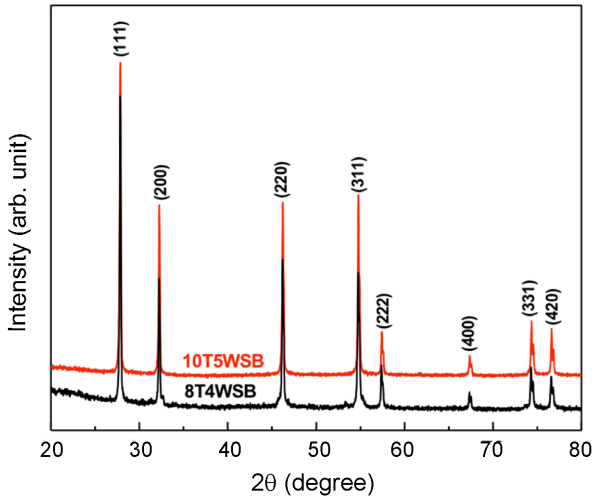

Fig. 5. XRD patterns of 8T4WSB and 10T5WSB.

than 20 mol%. Previously, Esaka and Iwahara reported a similar result with the TSB system.[20] However, the minimum dopant concentration in their study (> 30 mol% Tb) is higher than that of our result (~ 25 mol% Tb). Considering the meta-stable nature of the bismuth oxide phase at low dopant concentration, we attribute this deviation to different processing conditions during the calcination step along with different purities and morphologies of the initial powders.

The phase stability of 25TSB was observed using HT-XRD at the temperature range from 25 to 700°C. The resultant XRD patterns are plotted in Fig. 3, indicating that the cubic phase was retained from room temperature to higher temperatures up to 700°C, while a few minor impurity peaks were found at 700°C.

From the HT-XRD data, the lattice parameters of the 25TSB at various temperatures were calculated by the extrapolation method using the Nelson-Riley function with the following equations:[21]

$$a = a_0 + a_0 K\left(\frac{\cos^2\theta}{\sin\theta} + \frac{\cos^2\theta}{\theta}\right) \quad (1)$$

$$N = \frac{\cos^2\theta}{\sin\theta} + \frac{\cos^2\theta}{\theta} \quad (2)$$

where a, a_0, K, and N represent the apparent lattice parameter estimated from each peak position by Bragg's law, the true estimation of the lattice parameter, a constant, and the Nelson-Riley function, respectively. Fig. 4 shows the plots of the apparent measured parameters of 25TSB as a function of the Nelson-Riley function at 25, 300, 500, and 600°C. By extrapolation of each plot, the true lattice parameters (a_0) are 5.527, 5.546, 5.570, and 5.578 Å at 25, 300, 500, and 600°C, respectively. The calculated values increase as temperature increases, indicating the thermal lattice expansion of 25TSB.

Figure 5 shows the XRD results of 8T4WSB and 10T5WSB. Both compositions exhibit the crystal structure of the cubic fluorite, although 8T4WSB has some minor impurity peaks. These results clearly demonstrate that the double dopant strategy, which we previously used for the Dy and W co-doped Bi_2O_3 system, effectively drops the total dopant concentration to stabilize the cubic δ-Bi_2O_3 phase, thus expecting a higher conductivity with a lower total dopant concentration using a double dopant.

3.2. Conductivity

The conductivity of 25TSB and 10T5WSB was investigated via EIS measurement. Fig. 6 shows the resultant total conductivity as a function of inverse temperature for the measured samples in the temperature range from 300 to 700°C. For reference, we compared our results with the conductivity of 20 mol% Er-stabilized Bi_2O_3 (20ESB), and 8D4WSB from the literature,[19] which are known as the

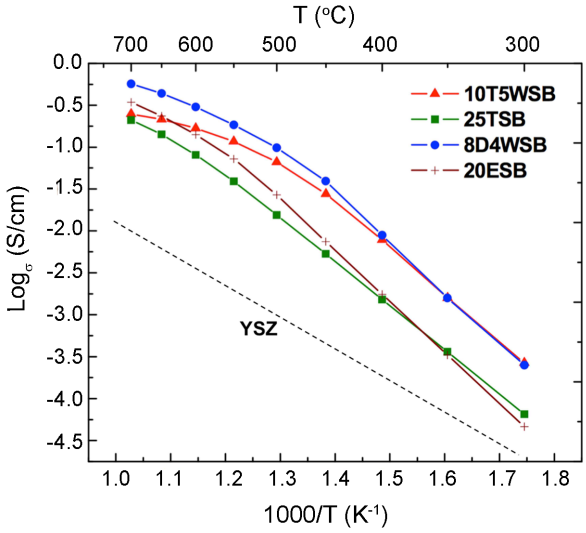

Fig. 6. Arrhenius plots of conductivities for 10T5WSB, 25TSB, 8D4WSB,[17] 20ESB,[19] and YSZ.[19]

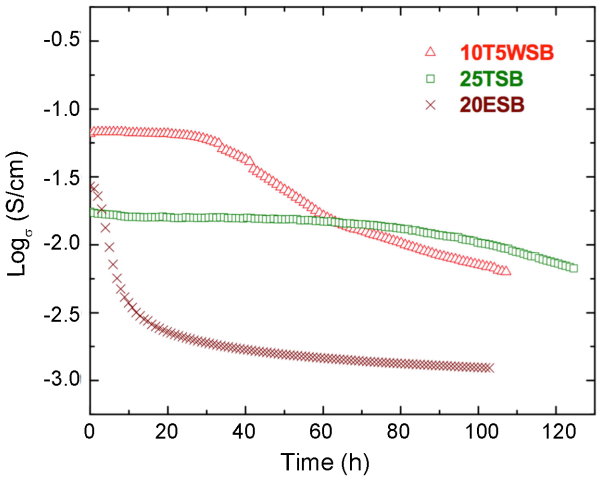

Fig. 7. Isothermal comparison of time-dependent conductivities of 10T5WSB, 25TSB, and 20ESB[19] annealed at 500°C.

highest conductivity compositions among the stabilized Bi_2O_3 systems with a single dopant and double dopants,[17] respectively. Based on previous studies, we believe that all these conductivities are primarily ionic conductivity, while further investigation is needed to confirm it. As shown in Fig. 6, the trend of the initial conductivities (σ) of these materials at temperatures between 400 to 600°C is clear:

$$\sigma(8D4WSB) > \sigma(10T5WSB) > \sigma(20ESB) > \sigma(25TSB).$$

For example, the ionic conductivity values of 8D4WSB, 10T5WSB, 20ESB, and 25TSB at 500°C are 0.0984, 0.0634, 0.0270, and 0.0155 S-cm^{-1}, respectively. This result is in good agreement with the previously reported theory that the ionic conductivity of stabilized bismuth oxides with the cubic fluorite structure strongly depends on the total dopant concentration irrespective of the kind of dopants used.[13,22]

However, below 400°C the initial conductivity of 25TSB is higher than that of 20ESB. This phenomenon is attributed to higher linearity of activation energy of 25TSB without significant change at the measured temperature ranges, while 20ESB showed a large activation energy change between 500 to 600°C due to order-disorder transition.[7] For co-doped 10T5WSB, its conductivity was lower than that of 20ESB and 8D4WSB at high temperatures (> 600°C), while it showed comparable conductivity at low temperatures (< 400°C).

3.3. Long-term stability

The long-term stability of 25TSB and 10T5WSB was investigated at 500°C for ~ 100 h. Fig. 7 shows the time-dependent conductivity behavior of 25TSB and 10T5WSB in addition to that of 20ESB from the literature[18] with the isothermal operation condition at 500°C in ambient air. We found that 25TSB has fairly good long-term stability compared with other compositions, even though its initial conductivity is relatively low while it experiences a small decrease in conductivity. The 10T5WSB sample has better initial conductivity than 20ESB and 25TSB due to its lower total dopant concentration as explained in the previous section, and it was considerably maintained for 35 h before gradual degradation occurred as a function of time. Therefore, we believe that, compared to 20ESB, larger dopants with high polarizability (Tb and/or W) are effective to suppress conductivity decay, as reported regarding other double-dopant (Dy and W)-stabilized bismuth oxides.[17-19]

The phase stability of TSB and TWSB was determined via XRD analysis after a long-term stability test at 500°C for ~100 h. Fig. 8 shows a comparison of the XRD patterns of 25TSB and 10T5WSB before and after annealing. The 25TSB sample experienced cubic to rhombohedral phase transformation (Fig. 8(a)), which may be attributed to the small decrease in conductivity after 80 h as shown in Fig. 7. For 10T5WSB, the cubic phase was fairly well maintained, but the crystallinity was considerably reduced (Fig. 8(b)).Thus, in this case, the major conductivity degradation mechanism could be the order-disorder transition[7] combined with possible non-crystalline phase formation. Moreover, further stability testing under various temperatures for longer operation periods should be conducted for the practical application of these novel electrolyte materials.

4. Conclusions

In this study, we developed and investigated new double-dopant stabilized bismuth oxides with Tb and W. With this double dopant strategy, the minimum dopant concentration to stabilize the cubic phase of bismuth oxides was effectively reduced. However, during long-term operation, TWSB showed a gradual decrease in conductivity and the crytallinity of its cubic phase was reduced. Thus, to develop novel SOFC electrolytes satisfying the demand for higher conduc-

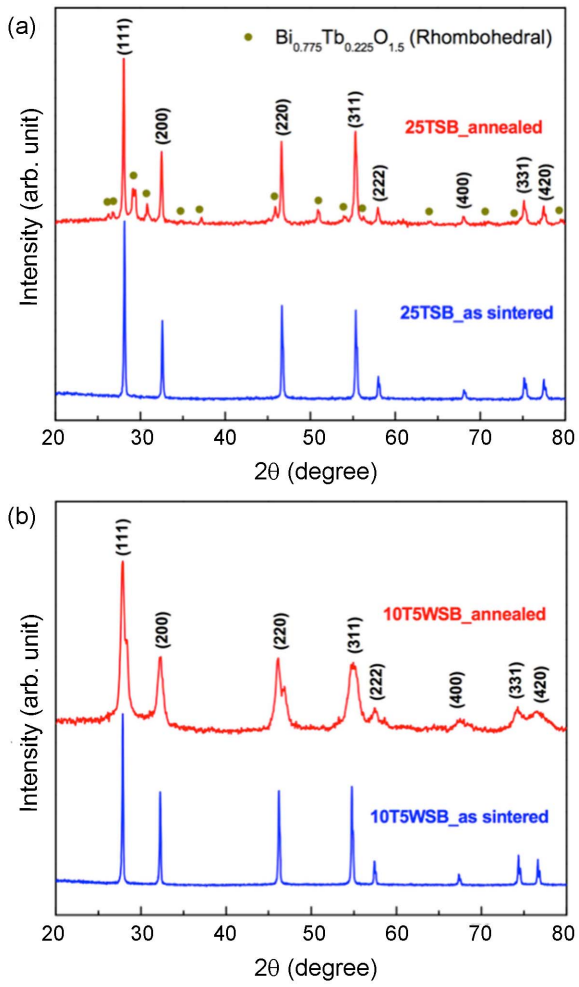

Fig. 8. XRD patterns of (a) 25TSB as-sintered and annealed at 500°C for 120 h and (b) 10T5WSB as-sintered and annealed at 500°C for 100 h.

tivity as well as better long-term stability at reduced temperature, further investigation of the degradation mechanism and composition optimization of TWSB system is in progress.

REFERENCES

1. E. D. Wachsman and K. T. Lee, "Lowering the Temperature of Solid Oxide Fuel Cells," *Science,* **334** [6058] 935-39 (2011).
2. B. C. H. Steele and A. Heinzel, "Materials for Fuel-cell Technologies," *Nature,* **414** [6861] 345-52 (2001).
3. K. T. Lee, H. S. Yoon, and E. D. Wachsman, "The Evolution of Low Temperature Solid Oxide Fuel Cells," *J. Mater. Res.,* **27** [16] 2063-78 (2012).
4. E. D. Wachsman, C. A. Marlowe, and K. T. Lee, "Role of Solid Oxide Fuel Cells in a Balanced Energy Strategy," *Energy Environ. Sci.,* **5** [2] 5498-509 (2012).
5. S. B. Adler, "Factors Governing Oxygen Reduction in Solid Oxide Fuel Cell Cathodes," *Chem. Rev.,* **104** [16] 4791-843 (2004).
6. S. Boyapati, E. D. Wachsman, and B. C. Chakoumakos, "Neutron Diffraction Study of Occupancy and Positional Order of Oxygen Ions in Phase Stabilized Cubic Bismuth Oxides," *Solid State Ionics,* **138** [3-4] 293-304 (2001).
7. E. D. Wachsman, "Effect of Oxygen Sublattice Order on Conductivity in Highly Defective Fluorite Oxides," *J. Eur. Ceram. Soc.,* **24** [6] 1281-85 (2004).
8. N. X. Jiang, E. D. Wachsman, and S. H. Jung, "A Higher Conductivity Bi_2O_3-based Electrolyte," *Solid State Ionics,* **150** [3-4] 347-53 (2002).
9. E. D. Wachsman, S. Boyapati, and N. Jiang, "Effect of Dopant Polarizability on Oxygen Sublattice Order in Phase-Stable Cubic Bismuth Oxide," *Ionics,* **7** [1-2] 1-6 (2001).
10. N. Q. Minh, "Ceramic Fuel-cells," *J. Am. Ceram. Soc.,***76** [3] 563-88 (1993).
11. T. Takahashi, T. Esaka, and H. Iwahara, "Electrical-conduction in Sintered Oxides of System Bi_2O_3-BaO," *J. Solid State Chem.,* **16** [3-4] 317-23 (1976).
12. T. Takahashi, T. Esaka, and H. Iwahara, "High Oxide Ion Conduction in Sintered Oxides of System Bi_2O_3-Gd_2O_3," *J Appl. Electrochem.,* **5** [3] 197-202 (1975).
13. M. J. Verkerk and A. J. Burggraaf, "High Oxygen Ion Conduction in Sintered Oxides of the Bi_2O_3-Dy_2O_3 System," *J. Electrochem. Soc.,* **128** [1] 75-82 (1981).
14. M. J. Verkerk, K. Keizer, and A. J. Burggraaf, "High Oxygen Ion Conduction in Sintered Oxides of the Bi_2O_3-Er_2O_3 System," *J. Appl. Electrochem.,* **10** [1] 81-90 (1980).
15. D. Mercurio, M. Elfarissi, B. Frit, J. M. Reau, and J. Senegas, "Fast Ionic-conduction in New Oxide Materials of the Bi_2O_3-Ln_2O_3-TeO_2 Systems (Ln = La, Sm, Gd, Er)," *Solid State Ionics,* **39** [3-4] 297-304 (1990).
16. G. Y. Meng, C. S. Chen, X. Han, P. H. Yang, and D. K. Peng, "Conductivity Of Bi_2O_3-based Oxide Ion Conductors With Double Stabilizers," *Solid State Ionics,* **28** [29-30] 533-38 (1988).
17. D. W. Jung, K. L. Duncan, and E. D. Wachsman, "Effect of Total Dopant Concentration and Dopant Ratio on Conductivity of $(DyO_{1.5})_X$-$(WO_3)_Y$-$(BiO_{1.5})_{1-X-Y}$," *Acta Mater.,* **58** [2] 355-63 (2010).
18. D. W. Jung, J. C. Nino, K. L. Duncan, S. R. Bishop, and E. D. Wachsman, "Enhanced Long-term Stability of Bismuth Oxide-based Electrolytes for Operation at 500°C," *Ionics,* **16** [2] 97-103 (2010).
19. D. W. Jung, K. L. Duncan, M. A. Camaratta, K. T. Lee, J. C. Nino, and E. D. Wachsman, "Effect of Annealing Temperature and Dopant Concentration on the Conductivity Behavior in $(DyO_{1.5})_x$-$(WO_3)_y$-$(BiO_{1.5})_{1-x-y}$," *J. Am. Ceram. Soc.,* **93** [5] 1384-91 (2010).
20. T. Esaka and H. Iwahara, "Oxide Ion and Electron Mixed Conduction in The Fluorite-type Cubic Solid-solution in The System Bi_2O_3-$Tb_2O_{3.5}$," *J. Appl. Electrochem.,* **15** [3] 447-51 (1985).
21. J. B. Nelson and D. P. Riley, "An Experimental Investigation of Extrapolation Methods in The Derivation of Accurate Unit-cell Dimensions of Crystals," *P. Phys. Soc. Lond.,* **57** [321] 160-77 (1945).
22. M. J. Verkerk and A. J. Burggraaf, "High Oxygen Ion Conduction in Sintered Oxides of the Bi_2O_3-Ln_2O_3 System," *Solid State Ionics,* **3-4** 463-67 (1981).